

Impact of Environmental Factors on LoRa 2.4 GHz Time of Flight Ranging Outdoors

Yiqing Zhou¹, Xule Zhou¹, Zecan Cheng¹, Chenao Lu¹, Junhan Chen¹, Jiahong Pan¹, Yizhuo Liu¹,
Sihao Li^{2,*}, and Kyeong Soo Kim^{1,*}

¹ School of Advanced Technology, Xi'an Jiaotong-Liverpool University, Suzhou, 215123, P.R. China.

Email: {Yiqing.Zhou24, Xule.Zhou23, Zecan.Cheng24, Chenao.Lu23, Junhan.Chen23, Jiahong.Pan22, Yizhuo.Liu23}@student.xjtlu.edu.cn, Kyeongsoo.Kim@xjtlu.edu.cn

² School of Artificial Intelligence, Suzhou Vocational Institute of Industrial Technology, Suzhou 215104, P.R. China.
Email: 01177@siit.edu.cn

Abstract—In WSN/IoT, node localization is essential to long-running applications for accurate environment monitoring and event detection, often covering a large area in the field. Due to the lower time resolution of typical WSN/IoT platforms (e.g., 1 μ s on ESP32 platforms) and the jitters in timestamping, packet-level localization techniques cannot provide meter-level resolution. For high-precision localization as well as world-wide interoperability via 2.4-GHz ISM band, a new variant of LoRa, called LoRa 2.4 GHz, was proposed by semtech, which provides a radio frequency (RF) time of flight (ToF) ranging method for meter-level localization. However, the existing datasets reported in the literature are limited in their coverages and do not take into account varying environmental factors such as temperature and humidity. To address these issues, LoRa 2.4 GHz RF ToF ranging data was collected on a sports field at the XJTLU south campus, where three LoRa nodes logged samples of ranging with a LoRa base station, together with temperature and humidity, at reference points arranged as a 3 \times 3 grid covering 400 m² over three weeks and uploaded all measurement records to the base station equipped with an ESP32-based transceiver for machine and user communications. The results of a preliminary investigation based on a simple deep neural network (DNN) model demonstrate that the environmental factors, including the temperature and humidity, significantly affect the accuracy of ranging, which calls for advanced methods of compensating for the effects of environmental factors on LoRa RF ToF ranging outdoors.

Index Terms—LoRa, wireless sensor network (WSN), Internet of Things (IoT), localization, environmental factors, ranging, time of flight (ToF), deep neural networks (DNNs).

I. INTRODUCTION

LoRa is one of the most popular technologies for low-power wide-area network (LPWAN), which can transmit data packets over several kilometers at low data rates with low-power consumption for a large variety of wireless sensor network (WSN)/Internet of Things (IoT) applications. Conventional LoRa implementations use a spread spectrum technology on license-free sub-GHz bands, which are different from one geographical region to another, resulting in many different parameter settings including frequency channel, maximum duty-cycle, and maximum transmission power. LoRa 2.4 GHz recently proposed by Semtech [1], on the other hand, uses the

common 2.4-GHz ISM band and thereby enables a worldwide coverage using a single platform without changing system parameters [2].

Of the several features of LoRa 2.4 GHz, the high-precision ranging implemented in Semtech's SX1280 chip can provide meter-level localization (i.e., up to 2 m) thanks to its use of radio frequency (RF) time of flight (ToF) [3], [4], which is not possible in conventional packet-level localization techniques due to the lower time resolution of typical WSN/IoT platforms (e.g., 1 μ s on ESP32 platforms) and the jitters in timestamping. The introduction of the high-precision RF ToF ranging could have a significant impact on the localization of WSN/IoT nodes deployed in wide areas; unlike the existing approaches for global positioning systems (GPS)-free geolocation based on LoRa, which suffer from low localization accuracy resulting from either conventional packet-level ToF or received signal strength (RSS)/received signal strength indicator (RSSI) fingerprinting, the GPS-free geolocation based on RF ToF could provide localization accuracy similar to or even better than that of GPS. Though the performance of Lora 2.4 GHz RF ToF ranging has been evaluated in terms of SX1280 transceiver parameter settings [5], the impact of environmental factors, like temperature and humidity, and their compensation techniques are yet to be fully investigated, which is important because LoRa nodes are typically deployed in outdoor environments.

In this paper, we present the results of our preliminary investigation of the impact of the environmental factors of temperature and humidity on the performance of LoRa 2.4 GHz RF ToF ranging outdoors, which is based on the ranging data collected together with temperature and humidity on a sports field at the XJTLU south campus over three weeks. We also explore the potential of compensating for the impact of environmental factors on LoRa RF ToF ranging based on a simple deep neural network (DNN) model.

The rest of the paper is organized as follows: Section II reviews related work. Section III describes our methodology for the investigation of LoRa 2.4 GHz RF ToF ranging. Section IV presents the results of our preliminary investigation based on the constructed database and a simple DNN model. Section V concludes our work.

* Corresponding authors.

II. RELATED WORK

A. GPS-Free Localization Techniques for WSN/IoT

WSN/IoT localization techniques not based on GPS can be grouped into those with and without ranging [6]. Ranging-based approaches rely on the distances between a node location and multiple anchor nodes with known locations or differences of them in determining the unknown node location through trilateration/multilateration. The ToF—also called time of arrival (ToA)—technique uses the travel time between a node location and anchor nodes [7], [8], while the time difference of arrival (TDoA) technique uses the time differences between the arrivals of the signals from a node at anchor nodes [7], [8]. Instead of arrival times or their differences, the angle of arrival (AoA) technique uses the angles of signal arrivals, which can be estimated by measuring time differences of arrivals between individual elements of an antenna array [9], [10].

In ranging-free localization techniques, a node location is not estimated based on distance-related information with trilateration/multilateration. In the case of *location fingerprinting*, the information measured at a node, e.g., RSSIs, channel state information (CSI), and geomagnetic field intensity, is used for localization, which is supposed to be unique to each location and thereby serves as a location fingerprint. RSSI fingerprinting, for example, has two operation phases of offline and online [11]: During the offline phase, the RSSIs at known locations, called reference points (RPs), are collected and stored in a fingerprint database; during the online phase, the node location is estimated based on the RPs whose RSSIs most closely match the newly-measured RSSIs at the node. In the case of Wi-Fi networks, CSI also can be used as location fingerprints, which, unlike coarse-grained RSSIs, can provide fine-grained indicators consisting of both amplitude and phase information during signal propagation and enables even single-access point (AP) localization. A significant drawback of CSI-based Wi-Fi fingerprinting, however, is the requirement of unique network interface cards (NICs) and device drivers for the acquisition of CSI (e.g., Intel 5300 NICs) [12].

B. RF ToF Ranging

As mentioned in Section I, the performance of the conventional packet-level ToF ranging is significantly limited by the lower time resolution of typical WSN/IoT platforms. With 1 μ s clock resolution, ToF distance estimate error can be up to 2000 m on LoPy4 development boards mounted on PyTrack sensor shields [13].

RF ToF ranging can address the limitation of the conventional ToF ranging and provide meter-level accuracy on comparable hardware platforms with little overhead of simple signal processing blocks [14]. In bandwidth limited systems like WSN/IoT, sub-clock ToF measurements can be done by resolving the phase offset of a signal. For example, pseudo-random noise (PN) codes can be used as signals for measuring small phase offsets because the autocorrelation function of a PN code exhibits a single large peak moving with a phase

offset, which is useful because a sequence of N values can be converted into a single feature with an effective signal to noise ratio (SNR) N times larger than that of the values used to construct it. The SNR enhancement is advantageous for noise limited ranging because interference from other signals, noise, or multipath propagation is a primary source of errors in RF ToF ranging [4].

III. METHODOLOGY

A network architecture for LoRa RF ToF ranging experiments is shown in Fig. 1, where an ESP32 board (i.e., WeMos D1 mini) facilitates wireless communication between end-users and LoRa nodes through a base station. While carrying out ranging, the LoRa nodes also capture temperature and humidity data using AHT20 sensors and log the measured data with corresponding timestamps and two-dimensional (2D) coordinates of RPs in a CSV file. A built-in web interface of the ESP32 board allows end-users to view live serial output and provides options to download or delete the CSV file. When Wi-Fi is unavailable, the time is calculated using the millis() function returning the number of milliseconds since the device was booted.

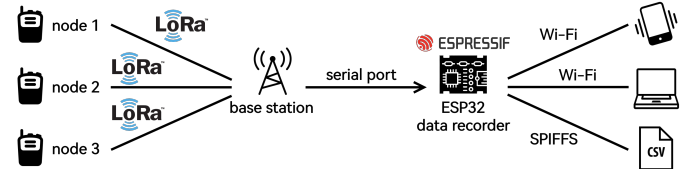


Fig. 1: A network architecture for LoRa RF ToF ranging experiments.

For distance measurements, the LoRa nodes use the SEMTECH SX1280-based transceiver at 2.4-GHz ISM-band, featuring an integrated RF ToF ranging engine. The ranging process involves a two-way exchange of packets between a LoRa node (i.e., a master) and a base station (i.e., a slave), measuring the round-trip time to estimate the distance. The SX1280 supports various configurations, including bandwidth, spreading factor, and coding rate, which can be adjusted to optimize performance based on environmental conditions. For our experiments, we apply the default settings for ranging applications.

IV. EXPERIMENTAL RESULTS

A. Experimental Setup

The RPs were established on a sports field at the XJTLU south campus as shown in Fig. 2. The nine red-circled RPs were located at one of 10-m grid points with the right lower RP as the origin of the coordinates, i.e., from (0, 0) to (20, 20), while the blue-circled base station was placed at (-10, -10).

Both a high-precision tape measure and a laser rangefinder were used for marking the RPs on the field to ensure positional accuracy.

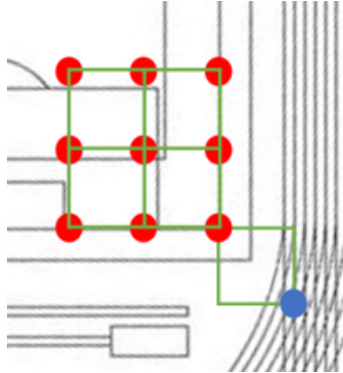


Fig. 2: The arrangement of RPs (red circles) and a base station (a blue circle) on a 10-m grid on a sports field at the XJTLU south campus.

For the experiments, four SX1280 LoRa evaluation boards were configured for RF ToF ranging; one of them was designated as the base station, and the other three were served as client nodes sequentially placed at each of the nine RPs to perform ranging measurements. As shown in Fig. 3, each evaluation board was mounted atop a rigid post approximately 40 cm high. This height was chosen to maintain consistency across measurements and to reduce potential signal interference from the artificial turf surface. Smartphones or laptops were used to download the collected data from the evaluation boards. About 1,000 distinct ranging measurements were recorded at each RP over a three-week observation period.



Fig. 3: A LoRa node deployed in the field for multi-range mass data acquisition.

B. Data Analysis

We first analyze the distribution of the LoRa RF ToF ranging errors over the RPs. For this purpose, we calculate the mean absolute ranging error at each RP after outlier handling, which is defined as

$$\bar{e}(x, y) = \frac{1}{N_{x,y}} \sum_{i \in \mathcal{G}(x,y)} e_i, \quad (1)$$

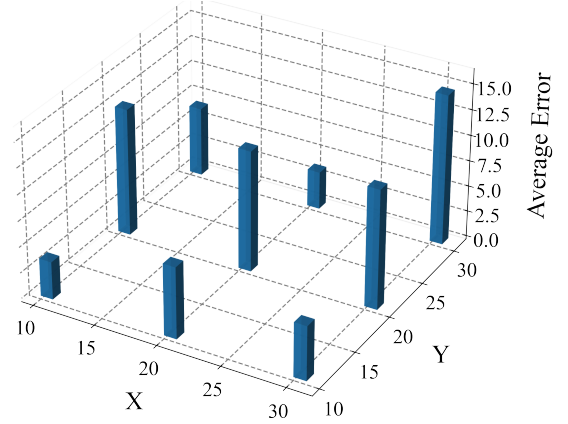


Fig. 4: A 3D bar chart of the mean of the absolute ranging errors at each RP.

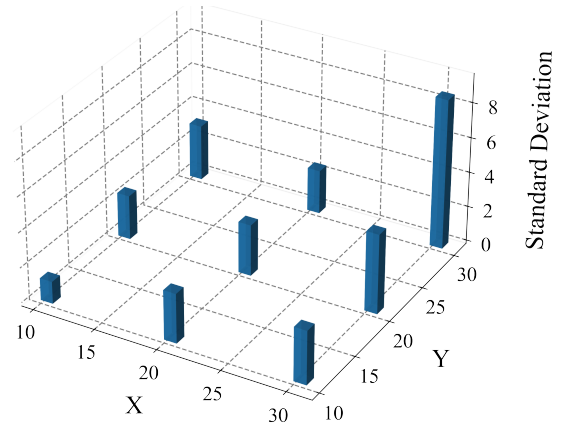


Fig. 5: A 3D bar chart of the standard deviation of the absolute ranging errors at each RP.

where $\mathcal{G}(x, y)$ denotes a set of records collected at an RP located at (x, y) , $N_{x,y}$ is its cardinality, and e_i is a per-record ranging error calculated as

$$e_i = |\text{Measured Distance}_i - \text{Ground-Truth Distance}_i|. \quad (2)$$

Note that the ground-truth distance in (2) is calculated based on the 2D coordinates of the RP and the base station.

As shown in Fig. 4, the three-dimensional (3D) bar chart of $\bar{e}(x, y)$ over all the RPs exhibit significant spatial variability of the mean absolute ranging errors across RPs, which indicates that geometrical and measurement conditions (e.g., relative orientation to the base station, blockage, and multipath) can affect the ranging errors.

We also quantify the stability of ranging at each RP using the standard deviation of the absolute ranging errors, which is shown in Fig. 5, where we can observe that the standard deviation at the RP located at (30, 30) is significantly greater than the others, indicating stronger fluctuations and thus poorer ranging stability at that RP; the minimum standard deviation of 1.27 m is observed at the RP located at (10, 10), while the majority of points fall in the 2.5–3.2 m range.

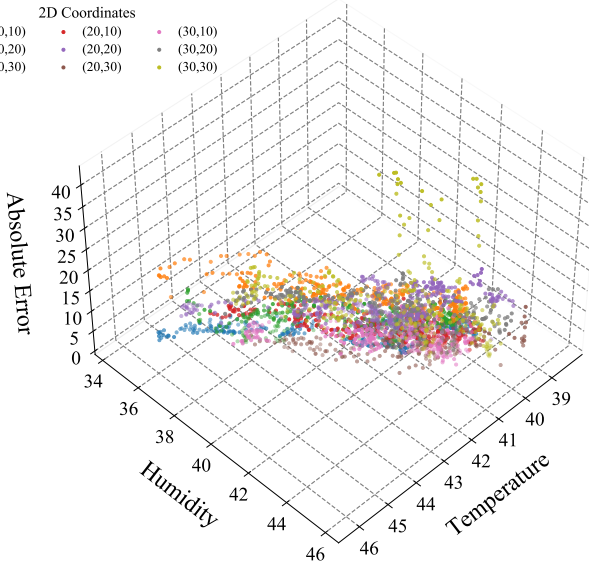


Fig. 6: A 3D scatter plot of temperature (X)-humidity (Y)-absolute ranging error (Z).

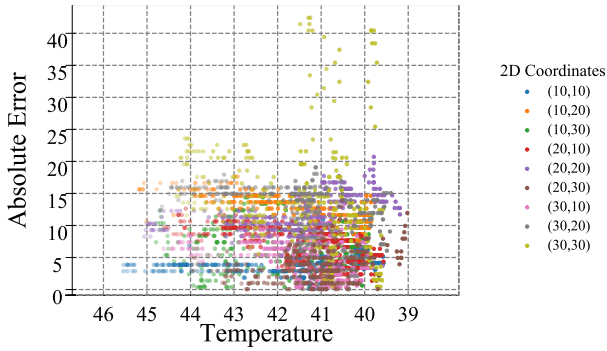


Fig. 7: Absolute ranging error vs. temperature.

To further investigate the impact of the environmental factors on LoRa RF ToF ranging based on the recorded environmental factors of temperature and humidity, we present a 3D scatter plot of temperature (X)-humidity (Y)-absolute ranging error (Z) colored and grouped by RP in Fig. 6 and its projection onto the X-Z and Y-Z planes in Figs. 7 and 8, respectively.

The points of the 3D scatter plot shown in Fig. 6 concentrate along the dimensions of temperature and humidity, instead of being randomly scattered. Also, when temperature or humidity increases, the absolute ranging errors at some RPs show a significant increase, and relatively concentrated “error bands” emerge in different ranges as shown in Figs. 7 and 8. This phenomenon indicates that temperature and humidity are correlated with the ranging errors, which suggests a potential of compensating for the impact of environmental factors on LoRa RF ToF ranging.

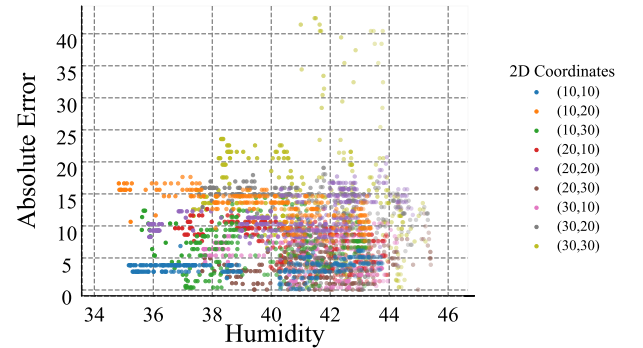


Fig. 8: Absolute ranging error vs. humidity.

C. Database Validation

The results of the data analysis presented in Section IV-B demonstrate that the ranging errors show a systematic dependence on environmental factors of temperature and humidity. To explore the potential of compensating for the impact of environmental factors on LoRa RF ToF ranging, we construct a simple DNN model whose input layer consists of two environmental features, temperature and humidity, and output layer corresponds to the absolute ranging error, thereby enabling an end-to-end mapping between environmental factors and error bias. The model architecture is composed of two fully-connected hidden layers and a regression output layer. During the training, the Adam optimizer and mean squared error (MSE) loss function are adopted to ensure stable convergence, while early stopping [15] and 5-fold cross-validation [16] are applied to enhance generalization performance. The hyperparameter values of the DNN model are summarized in Table I.

TABLE I: DNN hyperparameter values.

Parameter	Value
Input features	Temperature, Humidity
Output target	Absolute ranging error (m)
Hidden layers	Dense(128, ReLU), Dense(32, ReLU)
Output layer	Dense(1, Linear)
Optimizer	Adam
Learning rate	0.001
Loss function	MSE
Batch size	64
Max epochs	300
Early stopping patience	25

Table II shows the relatively stable results of the performance evaluation of the DNN model through 5-fold cross-validation, which provides the validation outcomes for each fold, including the MSE on the validation set, the denormalized mean absolute error (MAE), the root mean squared error (RMSE), and the coefficient of determination (R^2). The results indicate that under different environmental conditions, temperature and humidity exert varying impacts on the ranging error. Overall, the DNN model demonstrates good adaptability to diverse environmental settings. The mean values of MAE and

RMSE are 3.88 m and 5.03 m, respectively, further confirming that temperature and humidity significantly affect the ranging error, and that this impact can be efficiently compensated for by the DNN model to achieve “error correction.”

TABLE II: 5-fold cross-validation results.

Fold	val_MSE	MAE (m)	RMSE (m)	R^2
1	0.740044	3.689432	4.688753	0.116254
2	1.116877	4.217955	5.550302	0.079014
3	1.054927	4.130346	5.410613	0.105412
4	0.767498	3.654264	4.749471	0.137807
5	0.771699	3.692932	4.759478	0.140500
Mean	0.890209	3.876986	5.031723	0.115798
Std	0.161346	0.244585	0.369836	0.022609

V. CONCLUSIONS

In this paper, we have investigated the impact of the environmental factors of temperature and humidity on the performance of LoRa 2.4 GHz RF ToF ranging in an outdoor environment, which is based on the ranging data collected together with temperature and humidity on the sports field at the XJTLU south campus over three weeks.

Through the data analysis based on the 2D and 3D visualization of ranging errors, we identify not only a rather significant spatial variability of the mean absolute ranging errors across RPs but also a systematic dependence of absolute ranging errors on temperature and humidity. The results of the database validation based on a simple DNN model mapping between environmental factors and error bias, on the other hand, demonstrate a potential of compensating for the impact of environmental factors on LoRa RF ToF ranging, which call for advanced methods of compensating for the effects of environmental factors on LoRa RF ToF ranging outdoors.

ACKNOWLEDGMENT

This work was supported in part by Xi'an Jiaotong Liverpool University (XJTLU) Summer Undergraduate

Research Fellowships (under Grant SURF-2025-0217).

REFERENCES

- [1] semtech, “SX1280/SX1281 data sheet Rev 1.1,” May 2017.
- [2] G. H. Derévianckine, A. Guitton, O. Iova, B. Ning, and F. Valois, “Opportunities and challenges of LoRa 2.4 GHz,” *IEEE Commun. Mag.*, vol. 61, no. 10, pp. 164–170, Oct. 2023.
- [3] semtech, “Application note: An introduction to ranging with the SX1280 transceiver,” Mar. 2017.
- [4] S. Lanzisera, D. T. Lin, and K. S. J. Pister, “RF time of flight ranging for wireless sensor network localization,” in *Proc. WISES'06*. Vienna, Austria: IEEE, Jun. 2006.
- [5] F. Rander Andersen, K. Dilip Ballal, M. Nordal Petersen, and S. Ruepp, “Ranging capabilities of LoRa 2.4 GHz,” in *Proc. IEEE WF-IoT 2020*. New Orleans, LA, USA: IEEE, Jun. 2020, pp. 1–5.
- [6] S. He and S.-H. G. Chan, “Wi-Fi fingerprint-based indoor positioning: Recent advances and comparisons,” *IEEE Commun. Surveys Tuts.*, vol. 18, no. 1, pp. 466–490, First Quarter 2016.
- [7] S. A. Golden and S. S. Bateman, “Sensor measurements for Wi-Fi location with emphasis on time-of-arrival ranging,” *IEEE Trans. Mobile Comput.*, vol. 6, no. 10, pp. 1185–1198, 2007.
- [8] X. Chen, S. Song, and J. Xing, “A ToA/IMU indoor positioning system by extended Kalman filter, particle filter and MAP algorithms,” in *Proc. PIMRC 2016*, 2016, pp. 1–7.
- [9] F. Wen and C. Liang, “An indoor AOA estimation algorithm for IEEE 802.11ac Wi-Fi signal using single access point,” *IEEE Commun. Lett.*, vol. 18, no. 12, pp. 2197–2200, 2014.
- [10] J. Xiong and K. Jamieson, “ArrayTrack: A fine-grained indoor location system,” in *Proc. NSDI'13*, Lombard, IL, USA, 2013, pp. 71–84.
- [11] J. Xiao, Z. Zhou, Y. Yi, and L. M. Ni, “A survey on wireless indoor localization from the device perspective,” *ACM Comput. Surv.*, vol. 49, no. 2, pp. 1–31, Jun. 2016.
- [12] L. Zhang, E. Ding, Y. Hu, and Y. Liu, “A novel CSI-based fingerprinting for localization with a single AP,” *EURASIP Journal on Wireless Communications and Networking*, 2019.
- [13] J. Danebjer and V. Halldórsson, “A hybrid approach to GPS-free geolocation over LoRa,” Master’s thesis, Department of Electrical and Information Technology, Lund University, Lund, Sweden, Sep. 2018.
- [14] B. Thorbjørnsen, N. M. White, A. D. Brown, and J. S. Reeve, “Radio frequency (RF) time-of-flight ranging for wireless sensor networks,” *Measurement Science and Technology*, vol. 21, no. 3, p. 035202, Mar. 2010.
- [15] L. Prechelt, “Early stopping — but when?” in *Neural networks: Tricks of the trade: Second Edition*, G. Montavon, G. B. Orr, and K.-R. Müller, Eds. Springer Berlin Heidelberg, pp. 53–67.
- [16] Y. Bengio and Y. Grandvalet, “No unbiased estimator of the variance of k-fold cross-validation,” *J. Mach. Learn. Res.*, vol. 5, pp. 1089–1105, Dec. 2004.